European Journal of Medicinal Chemistry 47 (2012) 351–359

Contents lists available at SciVerse ScienceDirect

European Journal of Medicinal Chemistry

journal homepage: http://www.elsevier.com/locate/ejmech

Original article

Structure based drug design, synthesis and evaluation of 4-(benzyloxy)-1-phenylbut-2-yn-1-ol derivatives as 5-lipoxygenase inhibitors

Nimmanapalli P. Reddy [a], T. Chandramohan Reddy [a], Polamarasetty Aparoy [a], Chandrani Achari [a], P. Ramu Sridhar [b], Pallu Reddanna [a,*]

[a] School of Life Sciences, University of Hyderabad, Hyderabad 500 046, India
[b] School of Chemistry, University of Hyderabad, Hyderabad 500 046, India

ARTICLE INFO

Article history:
Received 8 July 2011
Received in revised form
13 October 2011
Accepted 1 November 2011
Available online 10 November 2011

Keywords:
4-(Benzyloxy)-1-phenylbut-2-yn-1-ol derivatives
5-LOX
Site point connection method
In silico prediction
Carcinoma cell line
Acute lung injury

ABSTRACT

A group of 4-(benzyloxy)-1-phenylbut-2-yn-1-ol derivatives were designed using Site point connection method, synthesized and evaluated for their 5-Lipoxygenase (5-LOX) inhibitory activity. Hydrophobic site points in 5-LOX were considered for the study and substitutions were planned such that **4k** will have strong hydrophobic group in the corresponding site point. Biological results supported the *in silico* prediction with compound **4k** exhibiting good inhibition with IC_{50} value of 8 μM against 5-LOX. The compounds **4j** and **4k** showed potent cytotoxic effects against various cancer cell lines (COLO-205, MDA-MB-231 and HepG2) but with no effect on normal cell line (HaCaT). The overall trend showed **4k** as the most potent compound. Further studies demonstrated the protective effect of **4k** in mouse Acute Lung Injury (ALI) model induced by lipopolysaccharide (LPS).

1. Introduction

Leukotrienes (LTs) are potent lipid mediators of inflammation [1]. The first step for LT biosynthesis requires 5-lipoxygenase (5-LOX), which, in the presence of 5-LOX-activating protein (FLAP), converts arachidonic acid into LTA_4 [2]. LTs have been implicated as inflammatory mediators in experimental models of acute lung injury (ALI) [3,4] and are known to contribute to the pathophysiology of osteoarthritis, asthma and other cancers including prostate, lung, breast and colon [5]. They were found to be elevated in pulmonary edema fluid obtained from patients with human acute respiratory distress syndrome (ARDS) [6]. MK886, a 5-LOX inhibitor has been shown to improve lung function by decreasing inflammatory parameters including LTB_4 induced by mechanical ventilation in a piglet model of airway lavage [7]. Recently, it has been shown that 5-LOX (ALOX5) is a critical regulator for leukemia cancer stem cells (LSCS) in chronic myeloid leukemia (CML) [8]. With an increase in reports illustrating the role of 5-LOX in various pathological conditions there is a growing demand for the development of potential and novel 5-LOX inhibitors [5]. In this study we focused on the development of 5-LOX inhibitors and their role in ALI.

ALI is a significant cause of morbidity and mortality in critically ill patients. Histologically, ALI in humans is characterized by a severe acute inflammatory response in the lungs and neutrophilic alveolitis [9,10]. Inflammatory stimuli from microbial pathogens, such as endotoxin [lipopolysaccharide (LPS)], are well recognized for their ability to induce pulmonary inflammation and experimental administration of LPS, both systemically and intratracheally, has been used to induce pulmonary inflammation in animal models of ALI [11–13], characterized by activation of alveolar macrophages, infiltration of neutrophils, lung edema and production of inflammatory mediators that resemble the inflammation and ALI seen in ARDS [14]. However, despite decades of research, few therapeutic strategies for clinical ARDS have emerged and current specific options for treatment are limited [15–17]. Studies suggest a causal role for 5-LOX and LTs in LPS-induced ALI [18,19]. It has been reported that mediators including LTB_4, are considered to be the major causes of ALI because of their strong effect on neutrophil activation and migration [20].

The increase in studies illustrating the role of 5-LOX in various diseases has increased interest in the development of

* Corresponding author. Tel.: +91 40 23134542; fax: +91 40 23010745.
E-mail addresses: prsl@uohyd.ernet.in, preddanna@yahoo.com (P. Reddanna).

0223-5234/$ – see front matter © 2011 Elsevier Masson SAS. All rights reserved.
doi:10.1016/j.ejmech.2011.11.003

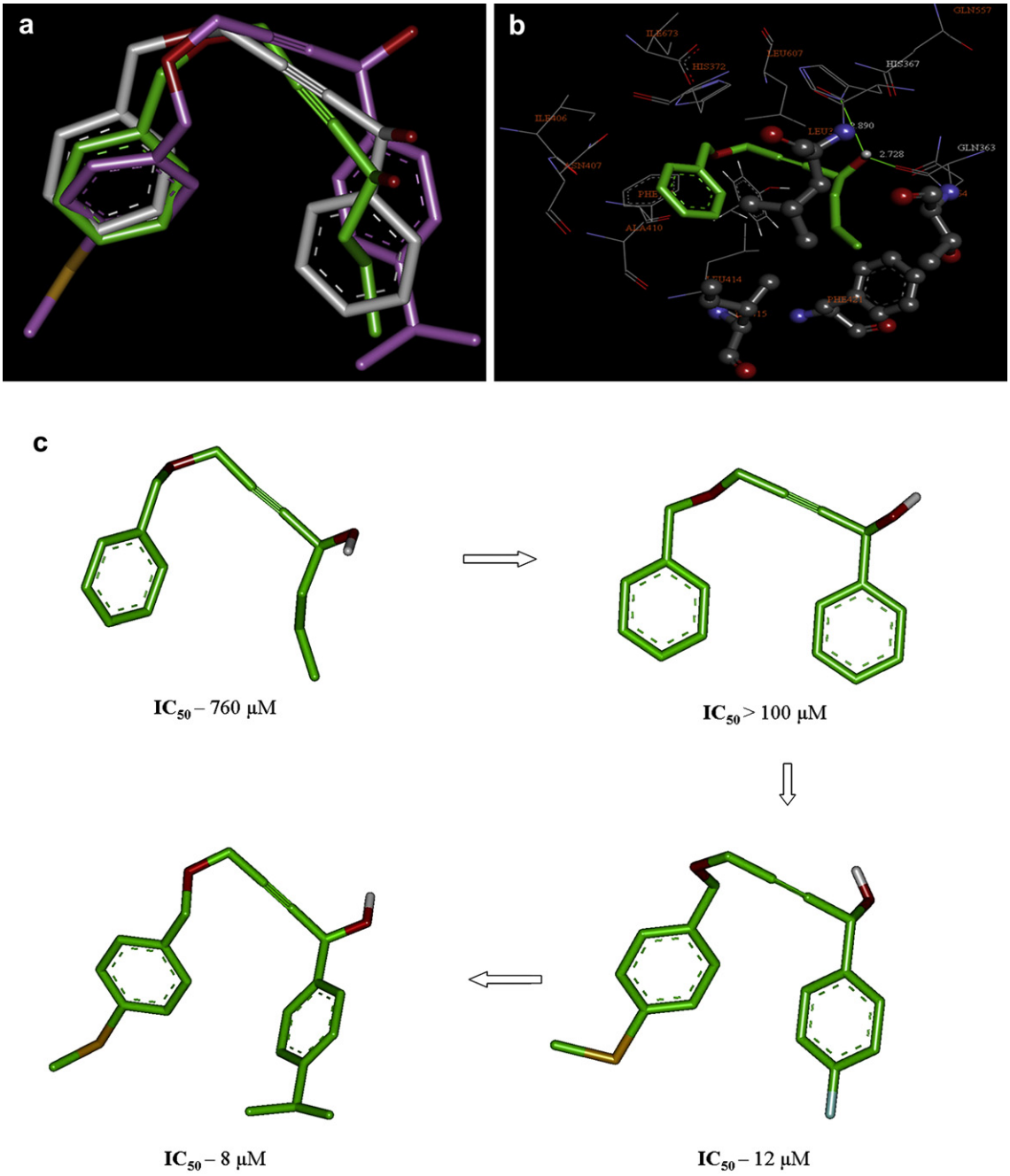

Fig. 1. (a) Overlay of best conformations BP-1, **4a** and **4k** (b) Interactions of BP-1 in 5-LOX active site; the hydrophobic amino acids in the vicinity are shown in ball and stick (c) Optimization of inactive molecule (IC_{50} – 760 μM) into active molecule (IC_{50} – 8 μM).

potential and novel 5-LOX inhibitors. There have been numerous reports recently on the synthesis and development of 5-LOX inhibitors [21–25]. In our earlier studies, we have reported a new class of inhibitors, prenylated chalcones [23] designed with the aid of a theoretical 3D model of potato 5-LOX elaborated by homology modeling [26]. Further, in another study, chemical feature based pharmacophore modeling of inhibitors of 5-LOX have been carried out. The fact that 5-LOX inhibitors can be successfully identified by employing pharmacophore based virtual screening explains its usefulness in predicting activities of large datasets of molecules. Thus, our earlier studies provided homology and pharmacophore models which help in designing the novel 5-LOX inhibitors. Further, in another study, we have performed 3D-QSAR, using the comparative molecular field analysis (CoMFA) and comparative molecular similarity indices analysis (CoMSIA) techniques to design molecules with better 5-LOX inhibitory activity [24]. As the crystal structure of human 5-LOX has been recently solved [27], it is now possible to employ the reliable structure for Structure Based Lead Optimization studies. It is well known that *de novo* design will rarely yield novel lead structures with nanomolar activity in the first instance. Rather, the designed structures will probably represent examples of a prospective new lead series with micromolar activities that require further optimization [28].

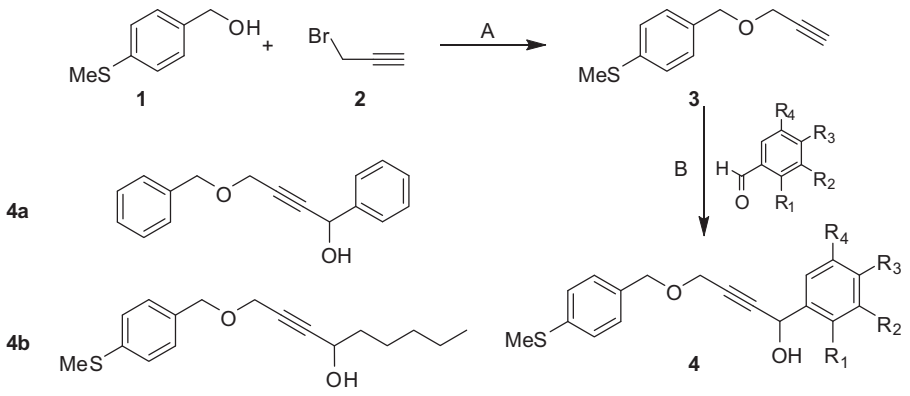

[a]Reagents and conditions: (A) DMSO, KOH, 0 °C to room temperature.

(B) THF, -78 °C n-BuLi, 3.5 h

	R_1	R_2	R_3	R_4
4c	H	H	OMe	H
4d	OMe	OMe	H	H
4e	OMe	OMe	OMe	H
4f	H	OMe	OMe	H
4g	H	OMe	OMe	OMe
4h	H	H	CN	H
4i	H	H	H	NO_2
4j	H	H	F	H
4k	H	H	^{i}Pr	H

Scheme 1. [a]Route for the synthesis of 4-(benzyloxy)-1-phenylbut-2-yn-1-ol derivatives.

As part of our ongoing search for potent 5-LOX inhibitors, we describe herein the design, synthesis and structure activity relationship (SAR) studies for new class of 4-(benzyloxy)-1-phenylbut-2-yn-1-ol derivatives as 5-LOX inhibitors. A study on single round lead optimization on 1-(benzyloxy) hept-2-yn-4-ol [(BP-1) (IC_{50} of 760 μM)] [29] was performed. Active site analysis method was employed to identify various important amino acids in the active site and Site Point Connection method was employed for lead optimization of an existing moderately active 5-LOX inhibitor. The designed molecules were synthesized and tested for 5-LOX inhibition *in vitro* and in the prevention of LPS-induced ALI in mouse model.

2. Results and discussion

2.1. Computational studies

Prior to the design of a 5-LOX inhibitor, the active site of 5-LOX was investigated. Because the 3D-structure of 5-LOX has been recently solved [27], it was used in this study. All of the possible ligand binding cavities on the 5-LOX were searched by the Binding Site Analysis program in Insight II. The largest cavity of 5-LOX obtained in Binding Site Analysis correlated with the inhibitor/substrate binding cavity of crystal structure of 15-LOX. This correlated well with the previous reports explaining the similarity in the structural fold and substrate/inhibitor binding site of LOXs. 5-LOX-benzyl propargyl ether complex was used as initial molecule for the lead optimization studies. The key regions in the active site that were essential for inhibitor binding were explored. The interaction sites in the vicinity of the inhibitor and unoccupied were identified. New leads were designed so that hydrophobic sites in the vicinity are exploited as shown in Fig. 1. The propyl group in BP-1 was replaced with phenyl group in compound **4a**. Further, methoxy, cyano, fluoro, isopropyl and nitro derivatives were designed and investigated (Fig. 1).

In the case of compound **4a**, most of the functional groups interacted favorably with the 5-LOX active site. Strong hydrogen bond interactions were observed between hydroxyl of compound **4a** and His367 (Nδ1···HO, 2.9 Å) and also with Gln363 (Oε1···HO, 2.8 Å). The Compound **4a** was expected to be more active than BP-1 as the substitution with the phenyl group favored stronger hydrophobic interactions with Leu368 and also much stronger Π–Π with Phe421.

In comparison, the conformation of active molecules **4j** and **4k** deviated little from **4a** because of the methylthio substitution. Unlike the hydrogen bond interactions seen in 5-LOX-**4a**, the thio derivatives formed strong interactions with Tyr181 and Gln363 (Fig. 1b). The phenyl group favored stronger hydrophobic interactions with Leu368 and also much stronger Π–Π with Phe421. The substitutions on the phenyl ring (thio, fluoro, cyano) occupied the site points adjacent to hydrophobic amino acids in the active site. Hence, the analogs were expected to be more active than **4a**. The substitutions in **4i**, **4j** and **4k** were planned such that the hydrophobicity of the functional group increases from **4i** to **4k**. Cyano, fluoro, isopropyl substitutions were made for **4i**, **4j** and **4k** respectively. This set of substitutions was used to again evaluate the site points identified. As all the substitutions occupy the same site point, the activity towards 5-LOX was expected to increase with increase in hydrophobicity of the functional group.

2.2. Synthesis

The synthetic strategies in this study to prepare the methyl ((4-(prop-2-ynyloxy) methyl) phenyl) sulfane is illustrated in Scheme 1.

Table 1
IC_{50} values of the compounds against 5-LOX enzyme.

IC_{50} (μM)	
Comp #	5-LOX
4a	>100
4b	>100
4c	>100
4d	69
4e	72
4f	80
4g	80
4h	41
4i	62
4j	12
4k	8
AA-861	1.7

Compound **3** was prepared by reacting 4-methylthiobenzyl alcohol with propargyl bromide and KOH in DMSO. The 4-(benzyloxy)-1-phenylbut-2-yn-1-ol derivatives **4b**–**k** were synthesized by generating the corresponding lithium acetalide of **3** using *n*-BuLi at −78 °C in THF followed by substituted aldehydes. The crude products were purified by column chromatography over silica gel. The structures of all the compounds were established on the basis of IR, ^1H, ^{13}C NMR and LCMS spectral data.

2.3. In vitro 5-LOX assay

The potential 5-LOX inhibitory molecules synthesized were tested *in vitro* for their inhibitory properties against 5-LOX enzyme using the assay described by Reddanna et al. (1990) [30]. Out of the ten molecules tested, compounds **4j** and **4k** showed inhibition at a concentration less than 15 μM. Compound **4h** and **4i** showed IC_{50} around 50 μM. All the other compounds showed IC_{50} greater than 100 μM. The most active molecule **4k**, showed potent inhibition of 5-LOX with an IC_{50} value of 8 μM (Table 1). The number of hydrogen bonds and hydrophobic interactions of the molecules with 5-LOX showed inverse correlation with the experimental IC_{50} values.

To elucidate the mechanism of action of compounds **4j** and **4k** on 5-LOX inhibition, assays were done as described by McGovern et al. (2002) [31]. IC_{50} values of the compounds **4j** and **4k** did not deviate upon incubation 5-LOX. Further, our results show that 5-LOX enzyme remained fully inhibited upon dilution of the mixture which suggested the binding is irreversible. Inhibition of 5-LOX by compounds **4j** and **4k** has showed negligible decrease (~1-fold) in the presence of 0.1 mg/mL BSA. These results suggest that inhibition of 5-LOX by compounds **4j** and **4k** is by a specific mechanism. To test whether the IC_{50} value of the compounds **4j** and **4k** altered upon increase in the concentration of 5-LOX, assays were carried by incubation of compounds with 5-fold and 10-fold excess of 5-LOX enzyme. These results showed a slight increase in the IC_{50} value with 5-fold increase in concentration of the enzyme, 5-LOX but with no change in IC_{50} value upon 10-fold increase in the concentration of 5-LOX (data not shown). The foregoing studies clearly demonstrate the specific and irreversible inhibition of 5-LOX by compounds **4j** and **4k**. A well-studied selective and competitive inhibitor of 5-LOX, AA-861 was not affected by incubation with the enzyme, 5-LOX.

2.4. In vitro anti-proliferative effects on cancer cell lines

The newly synthesized 4-(benzyloxy)-1-phenylbut-2-yn-1-ol derivatives were examined for their cytotoxic properties in three different human cancer cell lines; COLO-205 (colonic), HepG2 (hepatoma) and MDA-MB-231 (breast). The experiments were also carried out under the same experimental conditions in normal HaCaT (human keratinocyte) cell line. Cytotoxicity assays were carried out by using 3-(4, 5-dimethylthiazol-2-yl)-2, 5-diphenyl tetrazolium bromide (MTT) assay. The GI_{50} values calculated from the dose-survival curves obtained after 48 h of compound treatment from MTT assay are shown in Table 2. These results showed significant cytotoxic activity with compounds **4j** and **4k** against all the cell lines. In particular, compounds **4j** and **4k** were the most active agents against COLO-205 cell line with GI_{50} values of 22 and 12 μM respectively. Furthermore, compounds **4h** and **4i** showed moderate activity (<100 μM), the remaining compounds were less active towards COLO-205 cell line. Compounds **4j** and **4k** were also active against HepG2 and MDA-MB-231 cell lines as shown in the Table 2. No effect was observed on HaCaT cell line treated with **4j** and **4k** up to 100 μM (data not shown). These data suggest that **4j** and **4k** are compounds with potent cytotoxic effects on cancer cells but without any effect on normal cells.

Table 2
GI_{50} values of the compounds in various cell lines.

GI_{50} (μM)			
Comp #	COLO-205	HepG2	MDA-MB-231
4g	~100	~100	~100
4h	71	54	62
4i	88	91	81
4j	22	31	20
4k	12	22	15

2.5. In vivo anti-inflammatory effect of *4k* on LPS-induced ALI

2.5.1. *4k* Decreased LPS-induced inflammatory cells count and total protein concentration in the bronchoalveolar lavage fluid of ALI mice

Alveolar macrophages are one of the main sources of pro-inflammatory and anti-inflammatory cytokines, and their activation is critical in the development of ALI [32]. Total cell counts, differential cell counts and protein concentration in the bronchoalveolar lavage fluid (BALF) were evaluated at 12 h after LPS administration. In this study, as expected mice exposed to LPS exhibited massive recruitment of inflammatory cells, including neutrophils and macrophages to the airways. In contrast, pre-administration with **4k** at a single dose of 50 mg/kg, significantly inhibited the LPS-induced increase in the number of total cells, neutrophils and macrophages in the BALF [Fig. 2]. Similar results were obtained with celecoxib (CE) pre-treatment at a dose 50 mg/kg. Furthermore, LPS administration resulted in significant increase in the protein concentration in the BALF of mice. Pre-treatment with **4k** and CE at a single dose of 50 mg/kg each effectively reduced the protein concentration in the BALF. Thus, **4k** could attenuate LPS-induced ALI in mice by preventing infiltration of inflammatory cells and thus decreasing total protein concentration.

2.5.2. Effect of *4k* on LPS-induced pulmonary histopathological changes and W/D ratio

The effect of **4k** on the lungs of mice was determined 12 h after LPS administration by histochemical staining with H & E. As shown in Fig. 3a, LPS treated lungs showed pro-inflammatory alterations, characterized by alveolar wall thickening, massive infiltration of inflammatory cells into the lung interstitium and alveolar space as well as signs of tissue injury. In contrast, pre-treatment with a single dose of **4k** (50 mg/kg), 1 h before LPS challenge, markedly abated LPS-induced inflammatory cell infiltration and improved

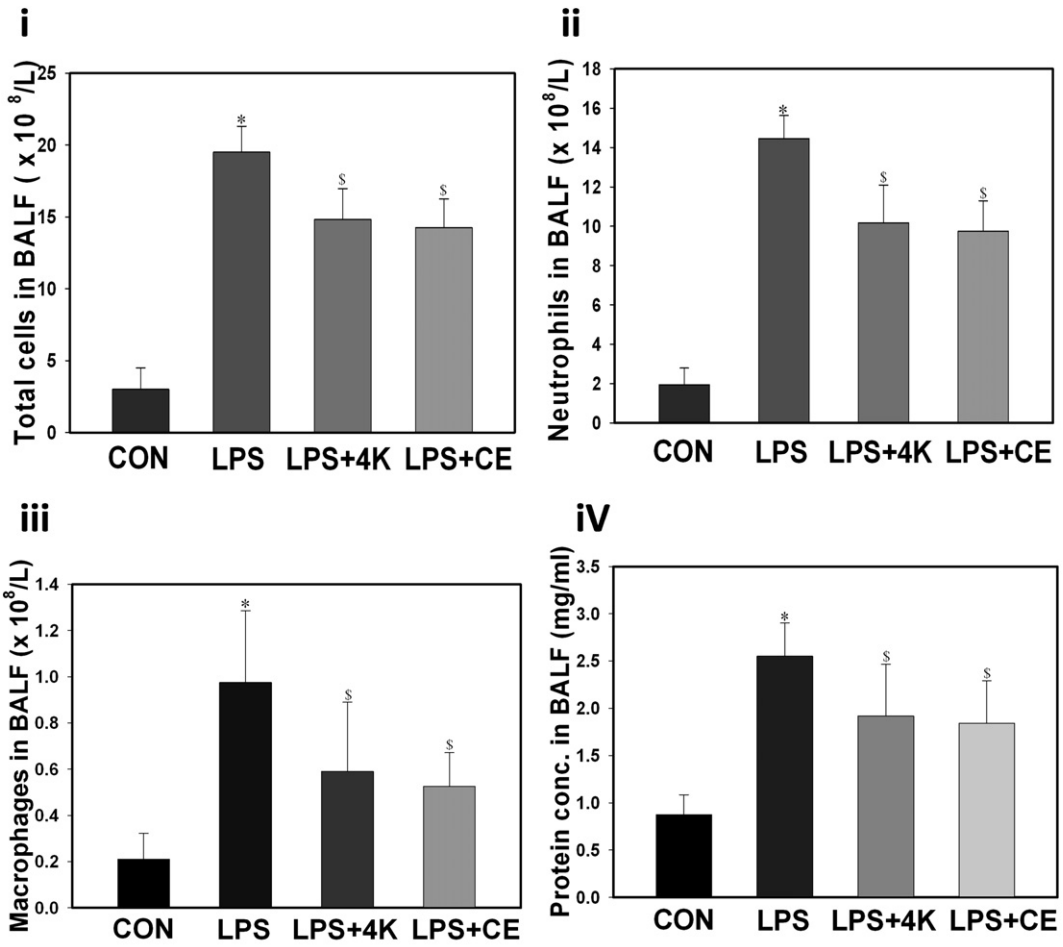

Fig. 2. Effects of **4k** on LPS-induced inflammatory cell accumulation and total protein in BALF. BALF was prepared from mice 12 h after LPS instillation and the total cell numbers (i) were counted using a standard hemocytometer. Each cell population including neutrophils (ii) and macrophages (iii) was examined by counting at least 200 cells on a smear prepared by Wright–Giemsa staining. The results are expressed as the cell numbers for each population in 1 L of BALF. (iv) Total protein level in the BALF was determined 12 h after the LPS challenge. $^{*}P < 0.01$ vs. control group; $^{\$}P < 0.05$ vs. LPS group.

alveolar wall thickening which was comparable with effects of 50 mg/kg dose of CE. The lung W/D ratio was evaluated as described in Materials and Methods. As shown in Fig. 3b, Compound **4k** significantly reduced the W/D ratio of lung 12 h after LPS instillation. These results corroborated our findings in BALF which confirmed that **4k** may attenuate LPS-induced pulmonary edema.

3. Conclusions

A new class of 4-(benzyloxy)-1-phenylbut-2-yn-1-ol derivatives have been designed, synthesized and evaluated for their 5-LOX inhibitory, anti-proliferative effects and *in vivo* anti-inflammatory effects. Prior to this work, structure based methods have not played a major role in the discovery of 5-LOX inhibitors, because experimental structures of 5-LOX do not exist. This study is a successful example reported for the 5-LOX inhibitor design using the *de novo* design strategy employing the recently solved crystal structure. A molecule of IC_{50} of 760 μM was optimized to a more potential molecule with IC_{50} of 8 μM. Site point connection method showed good promise and it can be further used in developing a very potential 5-LOX inhibitor. This methodology can be further used by exploiting other site points to yield novel lead structures with higher activity against 5-LOX enzyme.

4. Experimental section

4.1. Computational studies

Earlier we have reported the application of homology model of 5-LOX for the development of novel inhibitors [26]. The crystal structure of 5-LOX has been recently reported [22] and has been used in this Structure based lead optimization study of analogs of benzyl propargyl ether, a known class of 5-LOX inhibitors. BP-1, having IC_{50} of 760 μM [24] was used as the initial molecule for the design studies. The interactions of BP-1 with 5-LOX active site residues were thoroughly studied to understand the 5-LOX structure better.

The structure of the initial molecule was sketched and minimized using cerius2 and the final structure was obtained in conformational analysis. GOLD (Genetic Optimization of Ligand Docking), a docking program based on genetic algorithm [33] was used to dock the inhibitors. During docking, the default algorithm speed was selected. The number of poses for the inhibitor was set to 100, and early termination was allowed if the top three bound conformations of a ligand were within 1.5 Å RMSD.

After docking, the 5-LOX-BP-1 complex formed was studied. The interactions were visualized and important amino acids in the vicinity of the docked inhibitor were elucidated. Site point connection method is one of the most widely used ligand design

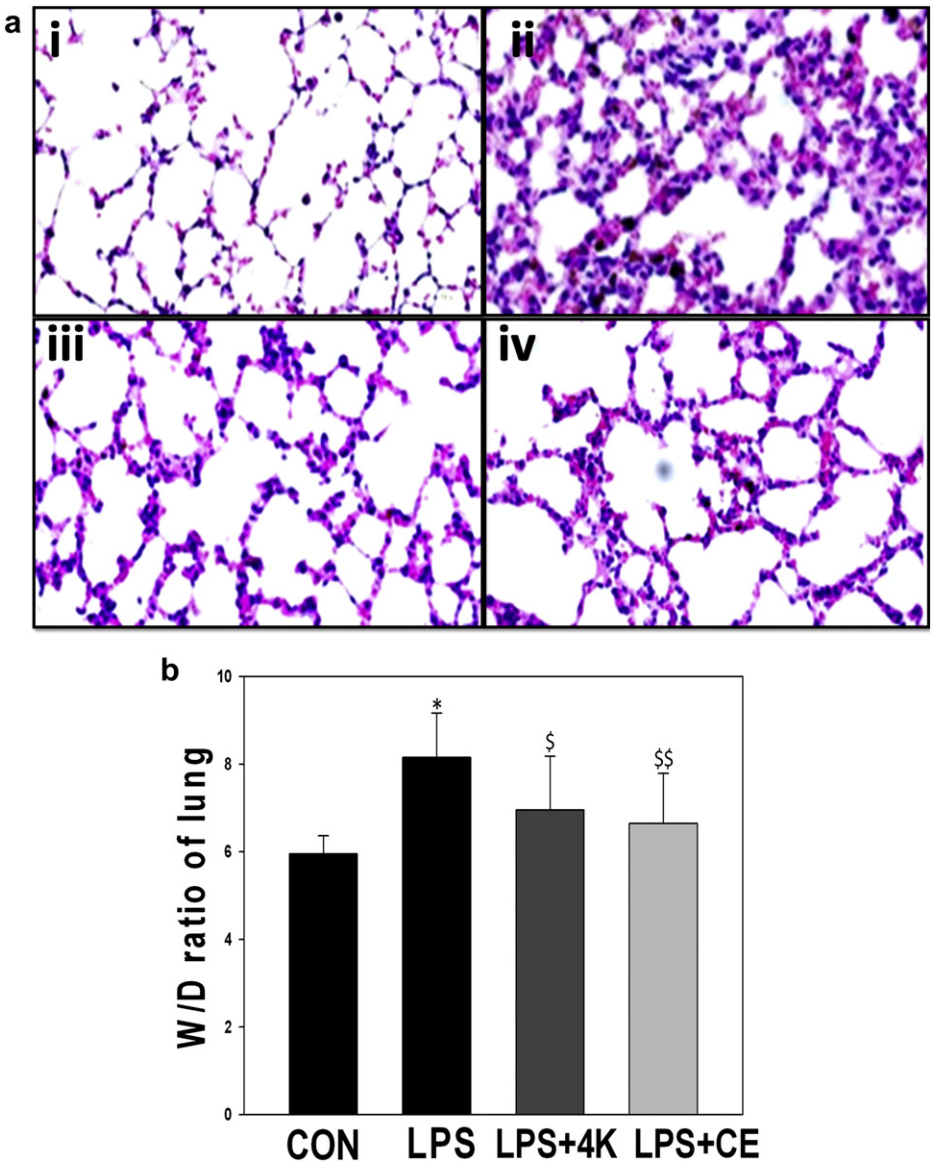

Fig. 3. (a) Histological assessment of the effect of **4k** on LPS-induced ALI. 12 h after LPS instillation, the lung tissues were inflated and fixed with 10% buffered formaldehyde; samples were embedded in paraffin, and then stained with H&E (400×). i. Control group; ii. LPS group; iii. **4k** group; and iv. CE group (b) Effects of **4k** on the lung W/D ratio of LPS-induced ALI in mice. To induce ALI, LPS was instilled intratracheally, 1 h after intra peritoneal administration of 50 mg/kg of **4k**. The lung W/D ratio (i) was determined 12 h after the LPS challenge. $^{*}P < 0.01$ vs. control group; $^{\$}P < 0.01$, $^{\$\$}P < 0.05$ vs. LPS group.

method. A site point can be defined as a space in the active site at which a suitable ligand atom can make favorable interactions with one or more enzyme atoms. Site points with appropriate ligand atoms nearby are said to be satisfied. Site point connection methods attempt to place small fragments in the active site so that one or more site points are satisfied and fragments are thereby placed in favorable regions.

The 5-LOX-benzyl propargyl ether complex discussed earlier was taken. With the knowledge of interaction sites in the 5-LOX obtained from active site analysis method, the site points that were in the vicinity of the docked inhibitor and were unoccupied by any of the ligand atoms were closely visualized. In this study, only the site points corresponding to hydrophobic interactions were considered. Four site points with potential of forming strong hydrophobic interactions were identified as Leu368, Ile415, Phe421 and Thr364 (Fig. 1b).

To exploit the hydrophobic amino acids round the active site, modifications of the ligand were proposed. All the molecules were docked and their interactions with 5-LOX were further investigated. Ten derivatives were designed using the design method taking the unsatisfied Site points into consideration. In the first step the aliphatic chain (propyl) was modified into aromatic ring (phenyl). The Compound **4a**, was designed and docked and investigated. The phenyl substitution leads to more hydrophobic interactions hence an increased affinity towards 5-LOX. To further exploit the surrounding amino acids, different substitutions were planned and studied.

4.2. Chemistry

4.2.1. General information

Melting points were determined on a Kofler hot-stage apparatus and are uncorrected. The reactions were monitored by thin layer chromatography (TLC) on precoated Merck Silica gel $60F_{254}$ aluminum plates. IR spectra were recorded in KBr discs on a JASCO FT/IR-5300. ^{1}H, ^{13}C NMR spectra were recorded on Bruker Avance

400 spectrometer using $CDCl_3$ with TMS as internal standard. Coupling constant (J) values are calculated in hertz (Hz) and spin multiples are given as s (singlet), d (double), t (triplet), q (quartet), m (multiplet) and br (broad). Elemental analyses were recorded on a Thermo Finnigan Flash EA 1112 analyzer. Column chromatography was performed on silica gel (Merk) 100–200 mesh.

4.2.2. Synthesis of methyl (4-((prop-2-ynyloxy) methyl) phenyl) sulfane (**3**)

To a suspension of KOH (16.8 g, 0.30 mol) in 100 mL DMSO was added 4-methylthiobenzyl alcohol (15.4 g, 0.10 mol). After stirring for 10 min, propargyl bromide (8.8 mL, 0.10 mol) was added at 0 °C. Stirring was continued for 3 h at room temperature. The resulting suspension was diluted with 200 mL water and was extracted with diethyl ether (3 × 100 mL). The combined organic layers were washed with water (4 × 60 mL), brine, dried over Na_2SO_4, filtered and concentrated under reduced pressure. The obtained yellowish residue was purified by silica gel column chromatography eluting with diethyl ether/hexane (2:8) to afford the title compound **3** as a colorless liquid (17.10 g, 89.0% yield).

^{1}H NMR (400 MHz, $CDCl_3$): δ 7.29 (d, J = 8.4 Hz, 2H), 7.25 (d, J = 8.4 Hz, 2H), 4.57 (s, 2H), 4.16 (d, J = 2.4 Hz, 2H), 2.48 (s, 3H, SMe), 2.47 (dd, J = 3.0 Hz, 1H); ^{13}C NMR (100 MHz, $CDCl_3$): δ 138.15, 134.00, 128.84, 128.58, 126.68, 126.41, 79.55, 74.62, 71.01, 56.89, 15.80.

4.2.3. General procedure for the synthesis of 4-(benzyloxy)-1-phenylbut-2-yn-1-ol derivatives

n-BuLi (1 mmol, 1.6 M in hexane) was added dropwise to a solution of propargyl benzyl ether (1.0 mmol) in freshly dried THF (10 mL) at −78 °C. The reaction mixture was stirred at −78 °C for 2.5 h, after that aldehyde (1.0 mmol) in dry THF (1 mL) was added dropwise. The reaction mixture was further stirred at the same temperature for 1 h and then allowed to warm to 25 °C over 30 min. After completion of reaction (by TLC) saturated aqueous NH_4Cl (10 mL) was added and the mixture was extracted with EtOAc (3 × 20 mL). The combined organic layers were dried over Na_2SO_4, filtered, and the solvent was evaporated in *vacuo*. The obtained crude product was purified by flash column chromatography over silica gel, eluting with step gradient of hexane/EtOAc to afford pure 1-Aryl-4-benzyloxybut-2-yn-1-ol derivatives **4b**–**k** with 70–80% yield. The reference compound **4a** was synthesized from the starting compound benzyl alcohol using the same procedure.

*4.2.3.1. 4-(Benzyloxy)-1-phenylbut-2-yn-1-ol (**4a**).* Pale Yellow oil (0.20 g); yield 80.0%; IR KBr ν_{max}: 3439, 3063, 2862, 2227 cm^{-1}. ^{1}H NMR (400 MHz, $CDCl_3$): δ 7.58–7.32 (m, 10H), 5.52 (s, 1H, CHOH), 4.62 (s, 2H, −OCH_2), 4.27 (d, J = 1.2 Hz, 2H, −OCH_2), 3.18 (br s, 1H, CHOH); ^{13}C NMR (100 MHz, $CDCl_3$): δ 140.59, 137.29, 128.68, 128.54, 128.42, 128.24, 128.02, 126.70, 86.68, 82.47, 71.75, 64.48, 57.47. Anal. ($C_{17}H_{16}O_2$): C, H.

*4.2.3.2. 1-(4-(Methylthio)benzyloxy)non-2-yn-4-ol (**4b**).* Yellowish oil (0.213 g); yield 72.9%; IR KBr ν_{max}: 3414, 2924, 2860, 1900 cm^{-1}. ^{1}H NMR (400 MHz, $CDCl_3$): δ 7.27 (d, J = 8.4 Hz, 2H, methylsulfanylphenyl H-2, H-6), 7.24 (d, J = 8.4 Hz, 2H, methylsulfanylphenyl H-3, H-5), 4.54 (s, 2H, −OCH_2), 4.42 (t, J = 6.4 Hz, 1H), 4.19 (d, J = 1.6 Hz, 2H, −OCH_2), 2.48 (s, 3H, SMe), 2.00 (s, 1H, CHOH), 1.72–1.68 (m, 2H), 1.48–1.44 (m, 2H), 1.33–1.30 (m, 4H), 0.90 (t, J = 6.4 Hz, 3H); ^{13}C NMR (100 MHz, $CDCl_3$): δ 138.12, 134.15, 128.68, 126.57, 87.81, 80.53, 71.10, 62.46, 57.24, 37.67, 31.40, 24.80, 22.52, 15.83, 13.96. Anal. ($C_{17}H_{24}O_2$ S): C, H.

*4.2.3.3. 1-(4-Methoxyphenyl)-4-(4-(methylthio)benzyloxy) but-2-yn-1-ol (**4c**).* Yellow gummy oil (0.244 g); yield 74.3%; IR KBr ν_{max}: 3398, 2920, 2852, 2227 cm^{-1}. ^{1}H NMR (400 MHz, $CDCl_3$): δ 7.47 (d, J = 8.0 Hz, 2H, methoxyphenyl H-2, H-6), 7.30–7.22 (m, 4H, methylsulfanylphenyl H-2, H-3, H-5, H-6), 6.90 (d, J = 8.0 Hz, 2H, methoxyphenyl H-3, H-5), 5.47 (s, 1H, CHOH), 4.65 (s, 2H, −OCH_2), 4.24 (d, J = 1.2 Hz, 2H, −OCH_2), 3.81 (s, 3H, −OMe), 3.10 (br s, 1H, CHOH), 2.48 (s, 3H, SMe); ^{13}C NMR (100 MHz, $CDCl_3$): δ 159.73, 138.20, 134.15, 132.76, 128.76, 128.08, 126.60, 114.00, 86.59, 82.39, 71.26, 64.24, 57.37, 55.36, 15.87. Anal. ($C_{19}H_{20}O_3$ S): C, H.

*4.2.3.4. 1-(2, 3-Dimethoxyphenyl)-4-(4-(methylthio)benzyloxy) but-2-yn-1-ol (**4d**).* Yellowish gummy oil (0.255 g); yield 71.2%; IR KBr ν_{max}: 3429, 2937, 2839, 2248 cm^{-1}. ^{1}H NMR (400 MHz, $CDCl_3$): δ 7.26–7.21 (m, 4H, methylsulfanylphenyl H-2, H-3, H-5, H-6), 7.12 (dd, J = 9.2, 1.6 Hz, 1H, dimethoxyphenyl H-6), 7.07 (t, J = 8.0 Hz, 1H, dimethoxyphenyl H-5), 6.91 (dd, J = 9.6, 1.6 Hz, 1H, dimethoxyphenyl H-4), 5.69 (s, 1H, CHOH), 4.54 (s, 2H, −OCH_2), 4.23 (d, J = 1.6 Hz, 2H, −OCH_2), 3.95 (s, 3H, −OMe), 3.88 (s, 3H, −OMe), 2.90 (br s, 1H, CHOH), 2.47 (s, 3H, SMe): ^{13}C NMR (100 MHz, $CDCl_3$): δ 152.55, 146.42, 138.01, 134.36, 134.12, 128.62, 126.51, 124.20, 119.40, 112.76, 86.71, 81.69, 71.06, 61.07, 57.29, 55.78, 15.78. Anal. ($C_{20}H_{22}O_4$ S): C, H.

*4.2.3.5. 4-(4-(Methylthio)benzyloxy)-1-(2, 3, 4-trimethoxyphenyl)-but-2-yn-1-ol (**4e**).* Pale yellow oil (0.273 g); yield 70.3%; IR KBr ν_{max}: 3433, 2939, 2841, 2247 cm^{-1}. ^{1}H NMR (400 MHz, $CDCl_3$): δ 7.24–7.18 (m, 5H, methylsulfanylphenyl H-2, H-3, H-5, H-6, trimetoxyphenyl H-6), 6.65 (d, J = 8.8 Hz, 1H, trimetoxyphenyl H-5), 5.61 (s, 1H, CHOH), 4.54 (s, 2H, −OCH_2), 4.23 (d, J = 1.6 Hz, 2H, −OCH_2), 3.99 (s, 3H, −OMe), 3.86 (s, 3H, −OMe), 3.85 (s, 3H, −OMe), 3.10 (br s, 1H, CHOH), 2.47 (s, 3H, SMe); ^{13}C NMR (100 MHz, $CDCl_3$): δ 154.04, 151.27, 142.01, 138.03, 134.10, 128.59, 126.66, 126.48, 122.11, 106.96, 86.68, 81.56, 71.05, 61.29, 60.94, 60.66, 57.29, 55.93, 15.75. Anal. ($C_{21}H_{24}O_5$ S): C, H.

*4.2.3.6. 1-(3, 4-Dimethoxyphenyl)-4-(4-(methylthio)benzyloxy) but-2-yn-1-ol (**4f**).* Yellowish gummy oil (0.254 g); yield 70.9%; IR KBr ν_{max}: 3352, 2935, 2841, 2222 cm^{-1}. ^{1}H NMR (400 MHz, $CDCl_3$): δ 7.25–7.19 (m, 4H, methylsulfanylphenyl H-2, H-3, H-5, H-6), 7.06–7.04 (m, 2H, dimethoxyphenyl H-2, H-6), 6.83 (d, J = 8.0 Hz, 1H, dimethoxyphenyl H-5), 5.45 (s, 1H, CHOH), 4.54 (s, 2H, −OCH_2), 4.23 (d, J = 1.6 Hz, 2H, −OCH_2), 3.86 (s, 6H, 2×−OMe), 2.71 (br s, 1H, CHOH), 2.45 (s, 3H, SMe); ^{13}C NMR (100 MHz, $CDCl_3$): δ 149.08, 138.22, 134.07, 133.19, 128.71, 126.57, 119.02, 110.93, 109.86, 86.66, 82.33, 71.23, 64.37, 57.36, 55.96, 55.89, 15.82. Anal. ($C_{20}H_{22}O_4$ S): C, H.

*4.2.3.7. (4-(methylthio)benzyloxy)-1-(3, 4, 5-trimethoxyphenyl)but-2-yn-1-ol (**4g**).* Pale yellowish oil (0.278 g); yield 71.6%; IR KBr ν_{max}: 3427, 2937, 2841, 2222 cm^{-1}. ^{1}H NMR (400 MHz, $CDCl_3$): δ 7.26–7.22 (m, 4H, metyhlsulfanylphenyl H-2, H-3, H-5, H-6), 6.77 (s, 2H, trimethoxyphenyl H-2, H-6), 5.45 (s, 1H, CHOH), 4.55 (s, 2H, −OCH_2), 4.23 (d, J = 1.6 Hz, 2H, −OCH_2), 3.85 (s, 3H, −OMe), 3.84 (s, 3H, −OMe), 3.83 (s, 3H, −OMe), 2.91 (br s, 1H, CHOH), 2.47 (s, 3H, SMe); ^{13}C NMR (100 MHz, $CDCl_3$): δ 153.25, 138.22, 137.85, 136.04, 133.94, 128.59, 126.50, 103.56, 86.30, 82.48, 71.21, 64.59, 60.77, 57.28, 56.06, 15.75. Anal. ($C_{21}H_{24}O_5$ S): C, H.

*4.2.3.8. 4-(1-Hydroxy-4-(4-(methylthio)benzyloxy)but-2-ynyl)benzonitrile (**4h**).* Yellowish oil (0.23 g); yield 71.2%; IR KBr ν_{max}: 3418, 3051, 2920, 2856, 2229, 2220 cm^{-1}. ^{1}H NMR (400 MHz, $CDCl_3$): δ 7.66 (d, J = 8.0 Hz, 2H, 4-cyanophenyl H-2, H-6), 7.63 (d, J = 8.0 Hz, 2H, 4-cyanophenyl H-3, H-5), 7.25–7.20 (m, 4H, methylsulfanylphenyl H-2, H-3, H-5, H-6), 5.55 (s, 1H, CHOH), 4.53 (s, 2H, −OCH_2), 4.22 (d, J = 1.2 Hz, 2H, −OCH_2), 2.91 (br s, 1H, CHOH), 2.47 (s, 3H, SMe); ^{13}C NMR (100 MHz, $CDCl_3$): δ 145.39, 138.45, 133.82, 132.43, 128.72, 127.17, 126.54, 118.61, 112.05, 85.32, 83.46, 71.58, 63.65, 57.28, 15.79. Anal. ($C_{19}H_{17}NO_2$ S): C, H, N.

*4.2.3.9. 4-(4-(methylthio)benzyloxy)-1-(3-nitrophenyl)but-2-yn-1-ol (**4i**).* Yellowish oil (0.242 g); yield 70.5%; IR KBr ν_{max}: 3400, 3084, 2922, 2860, 2235, 1529, 1350 cm^{-1}. ^1H NMR (400 MHz, $CDCl_3$): δ 8.40 (s, 1H, 3-nitrophenyl H-2), 8.17 (d, J = 8.0 Hz, 1H, 3-nitrophenyl H-4), 7.85 (d, J = 7.2 Hz, 1H, 3-nitrophenyl H-6), 7.54 (t, J = 8.0 Hz, 1H, 3-nitrophenyl H-5), 7.24–7.20 (m, 4H, methylsulfanylphenyl H-2, H-3, H-5, H-6), 5.59 (s, 1H, CHOH), 4.55 (s, 2H, $-OCH_2$), 4.24 (s, 2H, $-OCH_2$), 3.10 (br s, 1H, CHOH), 2.47 (s, 3H, SMe); ^{13}C NMR (100 MHz, $CDCl_3$): δ 148.33, 142.46, 138.42, 133.79, 132.64, 129.59, 128.74, 126.54, 123.25, 121.59, 85.31, 83.59, 71.58, 63.39, 57.25, 15.78. Anal. ($C_{18}H_{17}NO_4$ S): C, H, N.

*4.2.3.10. 1-(4-Fluoropylphenyl)-4-(4-(methylthio)benzyloxy) but-2-yn-1-ol (**4j**).* Yellow oil (0.226 g); yield 71.5%; IR KBr ν_{max}: 3398, 3074, 2920, 2856, 2222 cm^{-1}. ^1H NMR (400 MHz, $CDCl_3$): δ 7.50–7.46 (2H, m, 4-fluorophenyl, H-2, H-6), 7.27–7.19 (4H, methylsulfanylphenyl, H-2, H-3, H-5, H-6), 7.07–7.03 (m, 2H, 4-fluorophenyl, H-3, H-5), 5.46 (s, 1H, CHOH), 4.54 (s, 2H, $-OCH_2$), 4.22 (d, J = 1.2 Hz, 2H, $-OCH_2$), 3.10 (br s, 1H, CHOH), 2.47 (s, 3H, SMe); ^{13}C NMR (100 MHz, $CDCl_3$): δ 161.43, 138.33, 136.36, 133.92, 128.79, 128.53, 128.45, 126.56, 115.57, 115.35, 86.38, 82.61, 71.38, 63.75, 57.31, 15.79. Anal. ($C_{18}H_{17}FO_2$ S): C, H.

*4.2.3.11. 1-(4-Isopropylphenyl)-4-(4-(methylthio)benzyloxy) but-2-yn-1-ol (**4k**).* Pale yellowish oil (0.245 g); yield 72.0%; IR KBr ν_{max}: 3364, 3043, 2962, 2862, 2227 cm^{-1}. ^1H NMR (400 MHz, $CDCl_3$): δ 7.48 (d, J = 8.0 Hz, 2H, 4-isopropylphenyl H-2, H-6), 7.27–7.23 (6H, methylsulfanylphenyl H-2, H-3, H-5, H-6, 4-isopropylphenyl H-3, H-5), 5.50 (s, 1H, CHOH), 4.58 (s, 2H, $-OCH_2$), 4.26 (d, J = 1.2 Hz, 2H, $-OCH_2$), 2.94–2.92 [m, 1H, $CH(CH_3)_2$], 2.70 (br s 1H, CHOH), 2.47 (s, 3H, SMe), 1.30–1.26 [m, 6H, $CH(CH_3)_2$)]. ^{13}C NMR (100 MHz, $CDCl_3$): δ 149.34, 138.19, 137.89, 134.17, 128.78, 126.77, 126.70, 126.62, 86.56, 82.42, 71.26, 64.53, 57.37, 33.91, 23.99, 15.89. Anal. ($C_{21}H_{24}O_2$ S): C, H.

4.3. In vitro 5-LOX assays

5-LOX was purified and assayed by the method described by Reddanna et al. (1990) [30]. Enzyme activity was measured using polarigraphic method with a Clark's oxygen electrode on Strathkelvin Instruments, model 782, RC-300. Typical reaction mixture contained 50–100 μL of enzyme and 10 μL of substrate (133 μM of arachidonic acid) in a final volume of 3 mL with 100 mM phosphate buffer pH 6.3. Rate of decrease in oxygen concentration was taken as a measure of enzyme activity. Stock solutions of test compounds prepared immediately before use, were dissolved in DMSO. Various concentrations of test drug solutions were added and the LOX reaction was initiated by the addition of substrate. The reaction was allowed to proceed at 25 °C and the maximum slope generated was taken for calculating activity. Percent inhibition was calculated by comparison of LOX activity in the presence and absence of inhibitor. The concentration of the test compound causing 50% inhibition (IC_{50}) was calculated from the concentration-inhibition response curve. Each assay was repeated thrice.

To check whether the inhibition of the compounds **4j** and **4k** is irreversible and/or non-specific, assays were performed as described by McGovern et al. (2002) [31]. Compounds (**4j** and **4k**) and 5-LOX were incubated for 5 min at 25 °C at high concentrations (10-fold) and then diluted to below the apparent IC_{50} of the compounds **4j** and **4k** i.e. 12 μM and 8 μM. Then the reaction was initiated by the addition of AA (133 μM). Non-specific binding is often detected by decreased inhibition in the presence of BSA (MB083, Lot No. 0000090581, HiMedia, Mumbai, India). In order to check the non-specific binding, if any, in the present study, 5-LOX was incubated with BSA (0.1 mg/mL) and compounds **4j** and **4k** before addition of substrate and the reaction was initiated by the addition of AA (133 μM). In addition, 5-LOX inhibition, in the presence of 10-fold excess 5-LOX, 5-LOX and compounds **4j** and **4k** were incubated for 5 min and the reaction was initiated by the addition of AA (133 μM). A well-studied selective and competitive inhibitor of 5-LOX, AA-861 (A3711, Batch No. 036K1441, Sigma–Aldrich, St. Louis, USA) was used as a control in the assays.

4.4. MTT assay

Cell lines used in this study were maintained in tissue culture petri dishes. Medium for the cell line was RPMI-1640 supplemented with 10% heat inactivated fetal bovine serum (FBS) 100 IU/mL penicillin, 100 μg/mL streptomycin and 2 mM L-glutamine. The cell line was maintained in a humidified atmosphere with 5% CO_2 at 37 °C. The cultured cells were passaged twice a week, seeding at a density of 5×10^3 cells per well in 96-well plate before the day of experiment. Before the treatment with test compound, cells were washed with PBS and fresh medium was added. Cell proliferation was assessed using the MTT staining as described by Mosmann (1983) [34]. The MTT assay is based on the reduction of the tetrazolium salt, MTT, by viable cells. The NADH or NADPH generated in the living cells, convert the yellow form of the MTT salt to insoluble, purple formazan crystals. In brief, Cells (5×10^3 cells per well) were incubated in 96-well plates in the presence or absence of the test compounds (0.1–100 μM) for 48 h in a final volume of 100 μL. At the end of the treatment, 20 μL of MTT (5 mg/mL in PBS) was added to each well and incubated for an additional 4 h at 37 °C. The purple-blue MTT formazan precipitate was dissolved in 100 μL of DMSO. The activity of the mitochondria, reflecting cellular growth and viability, was evaluated by measuring the optical density at 570 nm on Quant Bio-Tek Instruments, Inc. microtiter plate reader. Each concentration was tested in three different experiments run in three replicates.

4.5. LPS-induced acute lung injury

4.5.1. Animals

Male BALB/c mice, weighing approximately 20–25 g, were purchased from the National Institute of Nutrition (NIN), Hyderabad, India. The mice were housed in micro isolator cages and received food and water *ad libitum*. The temperature was maintained at 24 ± 1 °C, and relative humidity was 40–80%. Mice were housed for 2–3 days to adapt them to the environment before experimentation. All animal experiments were performed in accordance with the guide for the Care and Use of Laboratory Animals published by the US National Institute of Health.

4.5.2. Chemicals

Escherichia coli lipopolysaccharide (LPS) was purchased from Sigma Chemical Company (St. Louis, USA). Celecoxib was a generous gift from Dr. Reddy's Laboratories, Hyderabad, India.

4.5.3. Establishment of the animal model and treatment regimen

The mice were divided randomly into a phosphate buffered saline (PBS) vehicle group (control group), an LPS challenge group (LPS group), a **4k** intervention group (**4k** group), and a Celecoxib intervention group (CE group), with 6 mice per group. After fasting for 8 h, mice were anesthetized with 50 mg/kg of ketamine and 10 mg/kg of xylazine in 100 μL of PBS, and 25 μg of LPS was administered intratracheally in 50 μL PBS (1 mg/kg), to induce lung injury. Control mice were given 50 μL PBS intratracheally. The mice were administrated **4k** at 50 mg/kg or CE at 50 mg/kg intraperitoneally, 1 h prior to LPS instillation; mice from control and LPS groups were treated with the same volume of PBS.

4.5.4. Bronchoalveolar lavage and Cell counting

Twelve hours after LPS or PBS instillation, BAL was performed three times through a tracheal cannula with 0.5 mL of autoclaved PBS, instilled up to a total volume of 1.3 mL. BALF was immediately centrifuged at 3000 rpm for 10 min (4 °C). The supernatants of BALF were stored at −70 °C until required for determination of protein content. The cell pellets were resuspended in PBS, and the total cell number was counted using a standard hemocytometer. Differences in cell numbers were examined by counting at least 200 cells on a smear prepared by Wright–Giemsa staining.

4.5.5. Wet-to-dry lung weight ratio

Twelve hours after the intratracheal instillation of LPS or PBS, left lungs were excised. Each lung was rinsed thrice in PBS, blotted dry, weighed, dried in an oven at 72 °C for 36–48 h, and re-weighed. The ratio of the wet lung to the dry lung was calculated to assess lung tissue edema.

4.5.6. Protein assay

Protein concentration in the supernatants of the BALF was measured using the Bradford assay [35]. Protein concentration was expressed as milligram per millilitre of BALF.

4.5.7. Histopathological analysis

Mice were anesthetised and killed 12 h after LPS administration, right lungs were removed and processed as follows: the lung tissues were inflated and fixed in 10% buffer formaldehyde, samples were embedded in paraffin, and then stained with hematoxylin and eosin (H&E). Evaluations of lung edema and inflammatory cell infiltration were performed under the light microscopy.

4.6. Statistical analysis

All values were expressed as the mean ± SEM. *P*-values were determined using the unpaired Student's *t*-test. *P* value of less than 0.05 was considered as statistically significant.

Acknowledgements

We thank Centre for Modeling, Simulation and Design (CMSD), University of Hyderabad for permitting us to use the computational facilities. We duly acknowledge the funding bodies UGC- Dr. D.S. Kothari PDF (N. Pulla Reddy, P. Aparoy), DBT-RA (T. Chandramohan Reddy) and CSIR (Chandrani Achari.) for providing financial support.

Appendix. Supplementary information

Supplementary data related to this article can be found online at doi:10.1016/j.ejmech.2011.11.003.

References

[1] R.A. Lewis, K.F. Austen, R.J. Soberman, N. Engl. J. Med. (1990) 645–655.
[2] O. Werz, D. Steinhilber, Pharmacol. Ther. 112 (2006) 701–718.
[3] T. Nagase, N. Uozumi, S. Ishii, K. Kume, T. Izumi, Y. Ouchi, T. Shimizu, Nat. Immunol. 1 (2000) 42–46.
[4] E.E. Moore, Claude H. Organ, Am. J. Surg. 200 (2010) 681–689.
[5] D. Wang, R.N. Dubois, Eicosanoids and cancer, Nat. Rev. Cancer 10 (2010) 181–193.
[6] M.A. Matthay, W.L. Eschenbacher, E.J. Goetzl, J. Clin. Immunol. 4 (1984) 479–483.
[7] T. Ankermann, A. Reisner, T. Wiemann, H. Koehler, M. Krams, M.F. Krause, Pediatric Pulmonol 41 (2006) 452–462.
[8] Y. Chen, Y. Hu, H. Zhang, C. Peng, S. Li, Nat. Genet. 41 (2009) 783–792.
[9] J.L. Mendez, R.D. Hubmayr, Curr. Opin. Crit. Care 11 (2005) 29–36.
[10] G.D. Rubenfeld, E. Caldwell, E. Peabody, J. Weaver, D.P. Martin, M. Neff, E.J. Stern, L.D. Hudson, N. Engl. J. Med. 353 (2005) 1685–1693.
[11] G. Matute-Bello, R.K. Winn, T.R. Martin, W.C. Liles, Clin. Diagn. Lab. Immunol. 11 (2004) 358–361.
[12] M. Rojas, C.R. Woods, A.L. Mora, J. Xu, K.L. Brigham, Am. J. Physiol. Lung Cell. Mol. Physiol. 288 (2005) L333–L341.
[13] C.W. Frevert, S. Huang, H. Danaee, J.D. Paulauskis, L. Kobzik, J. Immunol. 154 (1995) 335–344.
[14] K.L. Brigham, B. Meyrick, Am. Rev. Respir. Dis. 133 (1986) 913–927.
[15] D.M. Guidot, H.G. Folkesson, L. Jain, J.I. Sznajder, J.F. Pittet, M.A. Matthay, Am. J. Physiol. Lung Cell. Mol. Physiol. 291 (2006) L301–L306.
[16] M.A. Matthay, G.A. Zimmerman, C. Esmon, J. Bhattacharya, B. Coller, C.M. Doerschuk, J. Floros, M.A. Gimbrone Jr., E. Hoffman, R.D. Hubmayr, M. Leppert, S. Matalon, R. Munford, P. Parsons, A.S. Slutsky, K.J. Tracey, P. Ward, D.B. Gail, A.L. Harabin, Am. J. Respir. Crit. Care Med. 167 (2003) 1027–1035.
[17] D. Mehta, J. Bhattacharya, M.A. Matthay, A.B. Malik, Am. J. Physiol. Lung Cell. Mol. Physiol. 287 (2004) L1081–L1090.
[18] J. Palmblad, C.L. Malmsten, A.M. Uden, O. Radmark, L. Engstedt, B. Samuelsson, Blood 58 (1981) 658–661.
[19] K. Yoshimura, S. Nakagawa, S. Koyama, T. Kobayashi, T. Homma, J. Appl. Physiol. 76 (1994) 91–96.
[20] T.J. VanderMeer, M.J. Menconi, B.P. O'Sullivan, V.A. Larkin, H. Wang, M. Sofia, M.P. Fink, J. Appl. Physiol. 78 (1995) 1121–1131.
[21] P.N. Rao, Q.H. Chen, E.E. Knaus, J. Med. Chem. 49 (2006) 1668–1683.
[22] P.N. Rao, Q.H. Chen, E.E. Knaus, Bioorg. Med. Chem. Lett. 15 (2005) 4842–4845.
[23] N.P. Reddy, P. Aparoy, T.C. Reddy, C. Achari, P.R. Sridhar, P. Reddanna, Bioorg. Med. Chem. 18 (2010) 5807–5815.
[24] P. Aparoy, G.K. Suresh, K. Kumar Reddy, P. Reddanna, Bioorg. Med. Chem. Lett. 21 (2011) 456–462.
[25] C. Charlier, J.P. Henichart, F. Durant, J. Wouters, J. Med. Chem. 49 (2006) 186–195.
[26] P. Aparoy, R.N. Reddy, L. Guruprasad, M.R. Reddy, P. Reddanna, J. Comput. Aided Mol. Des. 22 (2008) 611–619.
[27] N.C. Gilbert, S.G. Bartlett, M.T. Waight, D.B. Neau, W.E. Boeglin, A.R. Brash, M.E. Newcomer, Science 331 (2011) 217–219.
[28] G. Schneider, U. Fechner, Nat. Rev. Drug Discov. 4 (2005) 649–663.
[29] N.B. Barhate, C. Madhava Reddy, P. Srinivasa Reddy, R.D. Wakharkar, P. Reddanna, Indian J. Biochem. Biophys. 39 (2002) 264–273.
[30] P. Reddanna, J. Whelan, K.R. Maddipati, C.C. Reddy, Methods Enzymol. 187 (1990) 268–277.
[31] S.L. McGovern, E. Caselli, N. Grigorieff, B.K. Shoichet, J. Med. Chem. 45 (2002) 1712–1722.
[32] J.M. Cavaillon, M. Adib-Conquy, Crit. Care Med. 33 (2005) S506–S509.
[33] G. Jones, P. Willett, R.C. Glen, A.R. Leach, R. Taylor, J. Mol. Biol. 267 (1997) 727–748.
[34] T. Mosmann, J. Immunol. Methods 65 (1983) 55–63.
[35] M.M. Bradford, Anal. Biochem. 72 (1976) 248–254.